Multichannel Analysis of Single-Turnover Kinetics of Cytochrome aa_3 Reduction of O_2

Salil Bose,[‡] Richard W. Hendler,*[,‡] Richard I. Shrager,[§] Sunney I. Chan,[||] and Paul D. Smith[⊥]

Laboratory of Cell Biology, National Heart, Lung, and Blood Institute, Physical Sciences Laboratory, Division of Computer Research and Technology, and Biomedical Engineering and Instrumentation Program, National Center for Research Resources, National Institutes of Health, Bethesda, Maryland 20892, and Arthur A. Noyes Laboratory of Chemical Physics, California Institute of Technology, Pasadena, California 91125

Received July 16, 1996; Revised Manuscript Received December 11, 1996[⊗]

ABSTRACT: The single-turnover kinetics of the oxidation of cytochrome aa_3 by O_2 have been studied using a new approach. Up to 1000 whole spectra covering both the Soret and α regions were sequentially collected at room temperature from single samples with a time resolution of 10 μs. All of the spectral and time information were used in analyses based on singular value decomposition. Four spectral transitions (i.e., intermediates) were distinguished with time constants near 0.01, 0.1, 1.1, and 30 ms. Two different kinds of sequential models were evaluated, one linear and the other branched. Although past kinetic analyses have emphasized the linear sequential model, the complexity of the intramolecular electron transfer in this enzyme suggests that a branched model be considered. This is especially true in a single-turnover experiment where earlier optical and EPR studies have pointed unequivocally to a branched model [Clore et al. (1980) *Biochem. J. 185,* 139−154; Blair et al. (1985) *J. Am. Chem. Soc. 107,* 7389−7399]. In the present study, analysis of spectral data in terms of the linear model did not reveal the formation and decay of the expected oxyferryl intermediate, whereas analysis of the branched model did. The results obtained using the branched model are consistent with all of the available evidence from a broad range of physical techniques that have been applied to examine the single-turnover kinetics of the oxidation of reduced cytochrome aa_3 by O_2.

The introduction of the flow-flash technique by Gibson and Greenwood in 1963 made possible the study of the rapid reactions of reduced cytochrome *c* oxidase with molecular oxygen at room temperature. In 1975, Chance and coworkers (1975a,b) introduced cryogenic techniques for slowing the kinetics of the reaction so that rapid measurements were not required. Both of these techniques stimulated considerable activity in various laboratories to try to understand the specific pathways and kinetics of the reaction so that a dependable model for the energy-transducing function of the enzyme could be formulated. Unfortunately, even after the 3 decades that followed the original breakthrough by Gibson and Greenwood, there is still no consensus on the detailed steps in the overall reaction sequence. In this paper, we introduce a new approach to resolve the complicated and overlapping combination of spectral changes that occur during the complete reaction. Specifically, we are able to collect up to 1000 sequential complete spectra that cover both the Soret and α absorbance regions of cytochrome aa_3 and to achieve a time resolution of 10 μs. The entire time sequence is followed on a single sample rather than on different samples for each time point with separate mixings, photolysis, and monitoring of the spectra as done previously [e.g., see Orii (1984, 1988) and Einarsdóttir et al. (1995)]. All of the accumulated spectral data are used in the analyses by singular value decomposition (SVD).

The deconvoluted spectral and kinetic data obtained from SVD were analyzed in terms of two different reaction models. We began with a linear series of sequential intermediates. Subsequently, a branched pathway was considered for the transfer of the third and fourth electrons to the bound oxygen intermediates. These two analyses led to very different conclusions for the reaction mechanisms of O_2 reduction. The linear sequential model yielded no clear-cut evidence for the current view that an oxyferryl component is a major intermediate in the pathway for the oxidation of fully reduced cytochrome aa_3 by O_2. In addition, all of the intermediates showed spectra for weakly or unliganded heme a_3.

The presence of the oxyferryl state has been supported by many laboratories using a variety of physical techniques, principally resonance Raman scattering and electron paramagnetic resonance (Chance et al., 1975b; Wikström, 1981, 1989; Orii, 1988; Babcock & Wikström, 1992; Blair et al., 1985; Han et al., 1990; Varotsis et al., 1993). One very serious experimental obstacle that could be responsible for the lack of clear support for the presence of the oxyferryl state in the spectral studies is the following. The primary spectral signature for the oxyferryl component is a broad positive peak in absorbance in the 570−580 nm region of the oxidized minus reduced absorption spectrum (Witt & Chan, 1987; Vygodina & Konstantinov, 1988). There are two unfortunate aspects of the experimental material under study. (1) The oxidized minus reduced absorption spectrum for cytochrome *a* also displays a broad positive peak in absorbance in the 570−580 nm region (reviewed in the Discussion section of this paper). (2) The magnitude of the

[‡] National Heart, Lung, and Blood Institute.
[§] Division of Computer Research and Technology.
[||] California Institute of Technology.
[⊥] National Center for Research Resources.
[⊗] Abstract published in *Advance ACS Abstracts,* February 1, 1997.

S0006-2960(96)01741-2 CCC: $14.00

expected oxyferryl absorption may not be large enough relative to that of the cytochrome *a* center to stand out, especially since the time constants for the oxidation of cytochrome *a* and the suspected formation of the oxyferryl intermediate are the same or very close to each other [this paper and Sucheta and Einarsdóttir (1996)].

The evidence for a branched model for electron flow from fully reduced cytochrome aa_3 to O_2 comes from electron paramagnetic resonance and optical spectroscopy studies at low temperature (Clore et al., 1980; Blair et al., 1985). Witt and Chan (1987) identified one of the 3-electron-reduced O_2 intermediates as an oxyferryl compound and the other as a ferrous Fe_{a_3}/cupric Cu_B hydroperoxide. We analyzed the collected kinetic and spectral data in terms of the proposed branched model and found that when the difference spectrum for the 90 μs component was considered in terms of the two intermediates postulated in the branched model rather than the single intermediate of the linear sequential model, there was an enhancement in positive absorbance in the 570−580 nm absorbance region for one of the branched intermediates relative to that obtained in the corresponding difference spectrum for the linear sequential model. Furthermore, the difference spectra for the other transitions corresponded to those predicted by the branched model. Because of the compatibility of the results of the analysis based on the branched model with the vast amount of work which supports the presence of the oxyferryl intermediate as opposed to the lack of clear support using the linear sequential model, we believe the branched model is more likely to be correct.

EXPERIMENTS AND COMPUTATIONS

General. Cytochrome aa_3 was isolated from beef heart by the method of Yoshikawa et al. (1977) as described in Pardhasaradhi et al. (1991). The turnover number determined both spectrophotometrically by cytochrome *c* oxidation and polarographically by O_2 uptake was 200 s^{-1} at pH 6.0 and 40−50 s^{-1} at pH 7.4, values comparable to other preparations tested under the same conditions (Wilms et al., 1980; Crinson & Nicholls, 1991; Malatesta et al., 1990; Ishibe et al., 1991; Hazzard et al., 1991; Morgan et al., 1989; Sinjorgo et al., 1986; Wrigglesworth, 1984). Expressed in terms of the units used by Caughey and co-workers (Einarsdottir et al., 1988), the activity was 25 units s^{-1} mg^{-1}/3 mL at pH 6.0 and 10 units s^{-1} mg^{-1}/3 mL at pH 7.4.

Spectrometer and Stopped-Flow Apparatus. A brief description of the spectrometer can be found in Hendler et al. (1993). A full description will appear separately. The spectrometer can collect up to 1024 sequential spectra with a programmable time resolution between spectra from 10 μs to 21 s. Two spectral ranges of 130 nm each with a spectral resolution of 2.9 nm can be selected and monitored simultaneously. The stopped-flow apparatus was a Model SF-2001 from KinTek Instruments, University Park, PA. This device initiates and stops rapid flow with a high torque stepping motor drive, rather than by an abrupt impact of pressure on the syringes, and eliminates the need for a stopping syringe. A system of copper tubing, stainless-steel tubing, gas-tight Hamilton valves, anaerobic bottles, and O_2 electrodes was attached to the apparatus, similar to that described for the Aminco Morrow stopped-flow apparatus used in our earlier publication (Hendler et al., 1993). This system was used to prepare anaerobic samples *in situ* prior to their direct transfer to the syringes of the stopped-flow device, as described below.

Optics and Laser. The monitor light source was a 400 W xenon arc lamp (Model 66083, Oriel Corp., Stratford, CT). The light was collected using an f1.5 condenser and passed through a water filter to remove heat. The collimated light was passed through two fast-acting shutters: an electromechanical shutter (Uniblitz Model V35S2, Vincent Associates, Rochester, NY) and a liquid-crystal shutter (Model LV100AC, Displaytech, Inc., Boulder, CO) controlled by a Model DR50 FLC driver (Displaytech, Inc.). The monitor light was subsequently focused on the proximal end of an optical fiber (General Fiber Optics, Cedar Grove, NJ) which conducted the light into the stopped-flow apparatus (optical path length 0.5 cm). The optical fiber was configured at the distal end (i.e., entry into the stopped-flow cell) into a square array (2 × 2 mm) to match the geometry of the stopped-flow cell. The transmitted light was collected with a second similarly matched optical fiber which was bifurcated at the distal end into two 3.9 × 0.5 mm rectangular patterns which conformed with the entrance slits of the high-speed optical multichannel analyzer monochromators.

The photolysis laser was the second harmonic of a pulse Nd:YAG (Model Surelite-10, Continuum, Santa Clara, CA) which produced 150 mJ, 5 ns wide pulses at 532 nm with a repetition frequency of approximately 10 Hz. The synchronization electronics associated with the data collection selected a single photolysis pulse from the repetitive pulse train. The laser flash was focused on the sample observation chamber in a direction perpendicular to the monitoring light path. A 530 nm holographic notch filter (HNF-532-1.0, Kaiser Optical Systems, Inc., Ann Arbor, MI) was used to prevent scattered actinic light from entering the monochromator. To reduce further any complications due to scattered actinic light, the wavelength range from 516 to 550 nm was not included in the analyses.

Experimental Protocol. Nitrogen gas (99.995%) was passed through one of the attached, empty reservoir bottles and its sidearm for 20 min to purge the system. Then 2.1 mL of 50 mM potassium phosphate buffer (pH 7.4) was introduced into the reservoir bottle through a hypodermic needle in a port at the top, and N_2 gas was bubbled through the solution until it was anaerobic (∼30 min), as indicated by the O_2 electrode. Then 22 or 44 μL of a stock solution of cytochrome aa_3 (0.45 M) was added through the top port and mixed with the anaerobic buffer by a rotating magnetic flea. The solution was then flushed with CO (Matheson purity) for 3 h in the dark. A tiny crystal of dithionite was placed at the bottom opening of a gas-tight, closed Hamilton syringe which was then attached to the top port. The anaerobic solution was taken into the syringe and then quickly replaced into the anaerobic bottle. CO flushing was continued for 30 min. This procedure resulted in the formation of a completely reduced CO-complexed enzyme as confirmed in a separate experiment using a DW2000 spectrophotometer (SLM Instruments, Inc., Urbana, IL). The enzyme complex was then transferred through the stainless-steel tubing to a syringe of the stopped-flow device. Air-equilibrated buffer was placed in the other syringe. The two solutions were mixed in a 1:1 ratio, producing final concentrations of close to 2.5 or 5.0 μM cytochrome aa_3.

For each kinetic experiment, a series of counter timers were used to control a precise series of events. First, a signal

was given to initiate the stopped-flow device. A delay of 25 ms ensued to allow for the slow 8-bit computer that controls the device to cycle through its programming information. Then a signal was given to open the mechanical shutter. A 15 ms delay was allowed for full opening of the mechanical shutter, but monitor light was prevented from reaching the reaction chamber of the stopped-flow device by the liquid-crystal shutter (LCS). It was important to protect the sample, because the relatively slow opening of the mechanical shutter could have produced a varying amount of premature photolysis of the CO-complexed enzyme. The LCS was opened in 30 μs by a signal which came 15 ms after the one which initiated the opening of the mechanical shutter. A signal to start data collection by activating the A/D converters was sent at the same time as the one to open the LCS. One millisecond later, the laser was fired. During the first 6.07 ms, spectra were taken every 10 μs to provide the highest density of information for the initial fast reaction steps. The collection schedule was then decreased to cover slower reactions that might be occurring. During the next 4 ms (to 10.07 ms), spectra were accumulated every 40 μs. Finally, to include possibly very slow conversions, spectra were taken every 1 ms out to 229 ms.

Analysis and Computations. The basic use of SVD to deconvolute overlapping spectral data that evolve during some change in conditions, such as a time course in a metabolic sequence, has been previously described (Hendler & Shrager, 1994). Briefly, the SVD procedure decomposes an input matrix of raw data which consist of columns of composite spectra and rows of kinetic information into three submatrices, one containing basis spectra, one containing weighting information in the form of singular values, and one containing basis vectors of kinetic changes. The kinetic vectors are "best-fitted" to a sum of exponentials to obtain fundamental kinetic constants and amplitudes for the changes occurring in each transition. The fitted constants and amplitudes are then used along with the singular values and basis spectra to deduce the individual difference spectra which correspond to each transition that is occurring. The time constants are the reciprocals of the kinetic constants. There are several aspects of the current use of SVD that are different from previous applications of the method as described in a recent review (Hendler & Shrager, 1994). These newer considerations will be briefly discussed here and presented in detail in supplemental material that is available upon request.

The kinetic traces of the difference spectra generated by SVD when fitted to a sum of exponentials apply most directly to a series of parallel decays of intermediates. Therefore, the difference spectra obtained may not correspond to distinct intermediates which would be present in a linear sequential model. If the sequential kinetic constants are sufficiently different from each other, both the parallel and linear sequential difference spectra will be essentially the same, but in cases where the constants differ by less than 10-fold, overlapping of adjacent spectra will be obtained (see supplementary material). The difference spectra for a branched sequence model are expected to be significantly different from those for either the parallel or the linear sequential models. The first step in applying an SVD approach to analyzing data in terms of the linear and branched sequential models is the same. The accumulated data are deconvoluted by SVD as described in the beginning of this section. It is important to stress that there is only one fitting process which applies to the testing of both the linear and branched sequential models. The statistics of the fittings and the basis spectra are identical for both models. The desired final difference spectra are obtained using suitable matrices of kinetic constants that are appropriate for each of the models, as demonstrated in the supplementary material.

The SVD method is able to recognize every change that is taking place in the sample material during the period of observation. This includes processes that may not be part of the sequential process of interest. In the current problem, we have found two kinetic processes that fall into this category. Cytochrome aa_3 is prepared for analysis by reducing an anaerobic, CO-flushed solution with a tiny crystal of dithionite. The dithionite sets the redox potential of the solution and is in a stoichiometric excess to the amount of cytochrome. Therefore, the subsequent air-oxidized enzyme is subject to a comparatively slow re-reduction by the excess dithionite. The kinetics of this process are mixed with the sequential kinetic process of interest. Because the actual amount of dithionite differs in each experiment, the kinetics of the re-reduction process also differ from experiment to experiment. SVD resolves this process, and provides both a kinetic constant (τ > 75 ms) and the expected difference spectrum. There is an additional extraneous kinetic process that we have observed from time to time. In experiment 238, this was seen at 2.0 ms, in experiment 274 at 7.0 ms, not at all in experiment 368, and at 7.9 ms in experiment 549. The difference spectrum for this process has the appearance of a reduction of CO-complexed enzyme.

In constructing the appropriate difference spectra for sequential events in both tested models, we have ignored the kinetic and spectral information related to the two extraneous processes that were separated by the SVD deconvolution. If this is not done, the unrelated spectral information could contaminate the spectra for the transitions of interest. The criteria used for accepting a transition as relevant to the enzyme kinetic model being tested were the following: (1) consistency in all experiments for the value of the kinetic constant and the resolved difference spectrum, (2) recognition that the difference spectrum showed coordinate redox changes consistent with the transfer of electrons from hemes *a* and a_3 either to each other or to O_2, and (3) the fact that the sum total of absorbance changes attributed to the oxidations of hemes *a* and a_3 added up to be close to the total changes expected for the amount of cytochrome aa_3 present. The kinetic constants and basis spectra for the four transitions that met all of the criteria were then used, as described in the supplementary material, to construct the difference spectra that are displayed in Figures 1, 5, and 6.

RESULTS

Analysis Based on a Linear Sequence of Intermediates. We depict first the turnover of the oxidase according to the linear sequential series of intermediates below, where the fully reduced starting species (y_1) is converted to the fully oxidized species (y_∞) through a series of unique sequential intermediates of progressively higher state of oxidation.

$$y_1 \xrightarrow{k_1} y_2 \xrightarrow{k_2} y_3 \xrightarrow{k_3} y_4 \xrightarrow{k_4} y_\infty$$

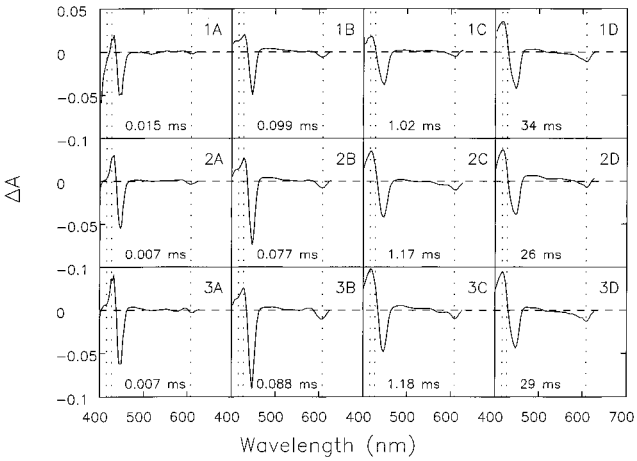

FIGURE 1: SVD-deduced difference spectra based on the linear sequential model. Each row shows the four kinetic transition difference spectra that were resolved by SVD from an averaged set of experimental data. For row 1, 17 experiments were averaged for a total time course of 207 ms. A total of 927 time points were employed as follows: 608 time points at 10 μs per point (0−6.07 ms), 100 points at 40 μs per point (to 10.07 ms), and 219 points at 0.9 ms per point (to 207 ms). The concentration of cytochrome aa_3 was 2.5 μM. For row 2, 33 experiments were averaged for a total time course of 229 ms. The first 708 time points were spaced as described above for row 1. The last 219 time points were spaced at 1 ms per point. The cytochrome aa_3 concentration was 5 μM. For row 3, 28 experiments were averaged. The time course and enzyme concentration were the same as for row 2. The number in each panel is the time constant for the transition as determined by SVD. Thus, the columns (A, B, C, and D) show the corresponding transition for the different averaged experiments. The vertical dotted lines in each panel denote the wavelength positions 416, 427, and 608 nm.

The subscripted k terms refer to the individual kinetic constants for each step.

Figure 1 summarizes SVD analyses of 78 separate kinetic experiments that consisted of a total of 4.77 million data points. Each experiment had 927 time-resolved spectra, consisting of 66 wavelengths which covered both the Soret and α absorptions of heme A. Each row in the figure represents an average of several experiments successively performed on the same day (viz., 17, 33, and 28 for rows 1, 2, and 3, respectively). In all cases, SVD resolved four kinetic steps involving the hemes, with time constants close to 0.01, 0.1, 1.1, and 30 ms. The resolved difference spectra for these transitions obtained with the linear sequential model are shown in columns A, B, C, and D, respectively. Figure 2 is similar to Figure 1, but instead of SVD-resolved spectra, actual difference spectra are shown for the time ranges that correspond to the time constants deduced in Figure 1. The SVD-resolved spectra represent the total amount of change for essentially isolated transitions (Hendler & Shrager, 1994). The actual difference spectra are contaminated with overlapping spectra from other transitions, they do not represent the total amount of spectral change, and they are noisier because they are not derived from all of the collected data. Nonetheless, they are useful because they verify the spectral transitions deduced by SVD.

The first transition shown in Figure 1 (column A) with a trough near 446 nm and a peak near 430 nm and a $\tau = \sim 0.01$ ms is consistent with the formation of an oxygenated heme a_3 complex, as first shown by Chance et al. (1975a,b). The next three transitions can be attributed to the oxidation of the reduced heme centers.

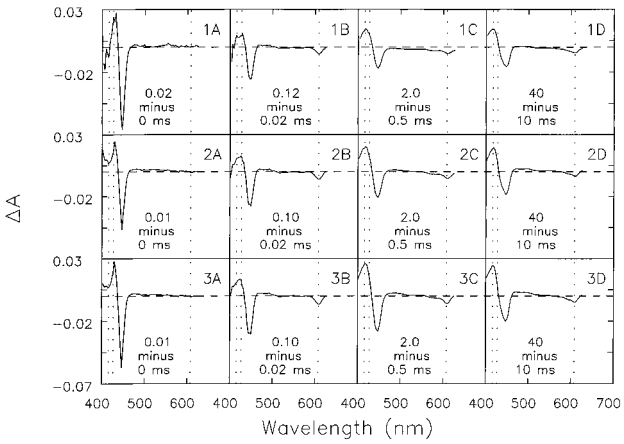

FIGURE 2: Actual difference spectra. Each panel in this figure relates to the corresponding panel in Figure 1. Whereas in Figure 1 the difference spectra and time constants were determined by SVD, in this figure actual difference spectra were generated from the raw experimental data. The times used for the difference spectra were chosen to reveal actual spectral changes taking place in a time frame which corresponds to the time constant shown in Figure 1. The vertical dotted lines in each panel denote the wavelength positions 416, 427, and 608 nm.

The different extents of cytochrome aa_3 oxidation during the kinetic studies displayed in Figures 1 and 2 are shown in Figure 3. Figure 3A shows the fully oxidized minus the dithionite-reduced difference spectrum for cytochrome aa_3 at a concentration of 5 μM. Figure 3B shows a difference spectrum for the oxidation 207 ms after the laser flash photolyzed the CO complex in experiment 238, in which 2.5 μM cytochrome aa_3 was present. Figure 3C,D shows the extents of oxidation which occurred during 230 ms of cytochrome oxidase oxidation in experiments 274 and 368, respectively, in which 5 μM cytochrome aa_3 was present. Quantification of the extent of oxidation during the taking of kinetic data was performed in two ways, one based on the ΔA (420−446 nm), and the other on the depth of the trough at 446 nm. Both methods yielded essentially the same results, namely, about 117, 70, and 82% for experiments 238, 274, and 368, respectively. An additional experiment consisting of 30 repeats with cytochrome aa_3 at 5.0 μM (549) yielded 92% oxidation. It is clear that the extents of CO-complexing, CO-photolysis, and cytochrome aa_3 oxidation were complete or nearly complete in all cases.

In Table 1, it is shown (experiments 274, 368, and 549) that the ΔA_{446} for the first oxidation step accounts for ∼50% of the total ΔA_{446} observed in the complete oxidation. These experiments include averages of 33, 28, and 30 individual experiments, respectively, each containing 5 μM cytochrome oxidase, whereas experiment 238 was an average of 17 experiments, each of which contained 2.5 μM cytochrome oxidase. The quantification obtained in experiment 238 is considered less reliable than that in the experiments which had greater signal and more data. In each of the next two resolved spectra, ∼25% of the total heme was oxidized. In the Discussion section, it is shown that the spectral changes obtained for the first oxidation step at 90 μs correspond very closely to those expected for the complete oxidation of heme a whereas the two later oxidation steps correspond very closely to those expected for the complete oxidation of heme a_3.

Analysis Based on a Branched Sequence Model. Earlier work by Clore et al. (1980) and Blair et al. (1985) has shown

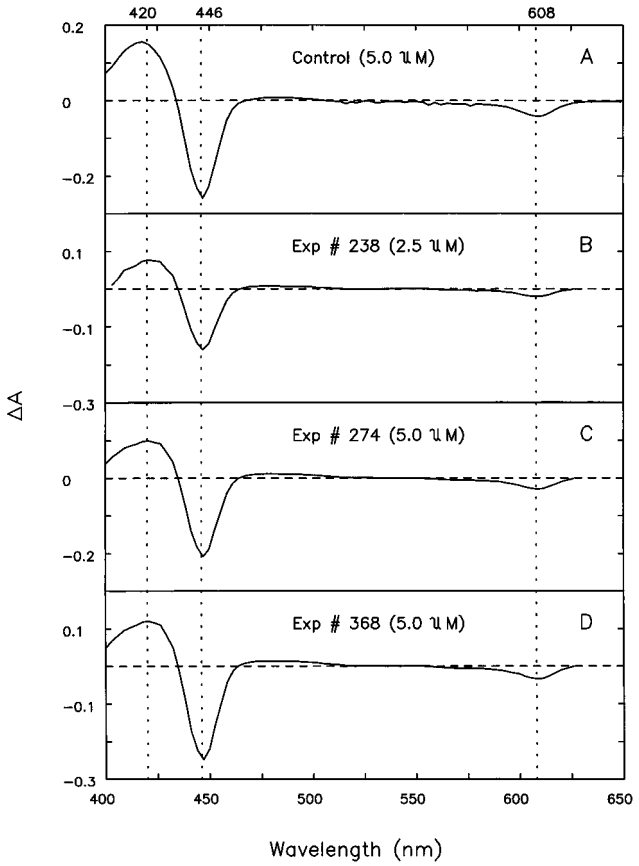

FIGURE 3: Quantification of extents of enzyme oxidation. Panel A shows a resting oxidized minus dithionite-reduced difference spectrum for 5 μM cytochrome aa_3. Panel B shows the difference spectrum for the last (207 ms) minus the first (0 ms) spectra in the averaged experiment 238 in which 2.5 μM cytochrome aa_3 was present. Panel C shows the difference spectrum for the last (229 ms) minus the first (0 ms) spectra in the averaged experiment 274 in which 5.0 μM cytochrome aa_3 was present. Panel D shows the difference spectrum for the last (229 ms) minus the first (0 ms) spectra in the averaged experiment 368 in which 5.0 μM cytochrome aa_3 was present.

that the peroxy intermediate can accept a third electron from either heme *a* or Cu_A. This results in a branched pathway leading from the 2-electron-reduced species to the fully reduced product. Witt and Chan (1987) identified the two 3-electron reduced intermediates as an oxyferryl and a ferrous heme a_3, cupric, hydroperoxide. The branched model proposed by Chan and his co-workers (Blair et al., 1985; Witt & Chan, 1987) is adapted for the present analysis in Figure 4. The kinetic scheme for the model is

$$y_1 \xrightarrow{k_1} y_2 \xrightarrow{k_2 f_3} y_3 \xrightarrow{k_3} y_\infty$$

$$y_1 \xrightarrow{k_1} y_2 \xrightarrow{k_2 f_4} y_4 \xrightarrow{k_4} y_\infty$$

Here, the starting fully reduced state (y_1) reaches the fully oxidized state (y_∞) via two pathways, one passing through the partially oxidized intermediate (y_3) and the other passing through the intermediate y_4. The subscripted *k* terms represent the kinetic constants for each step, while f_3 and f_4 are the fractions of y_2 going through y_3 and y_4, respectively. As a first attempt in using this model, and in the absence of reliable information on the values of f_3 and f_4 at room temperature, it will be assumed that $f_3 = f_4 = 0.5$. The

Table 1: Extents of Heme Oxidation for Each Kinetic Step

kinetic step	expt no.	concn (μM)	ΔA_{446}	%[a]
$\tau_1 = \sim 0.09$ ms	238[b]	2.5	0.050	38
	274	5.0	0.073	48
	368	5.0	0.090	50
	549	5.0	0.094	46
$\tau_2 = \sim 1.1$ ms	238	2.5	0.038	29
	274	5.0	0.041	27
	368	5.0	0.047	26
	549	5.0	0.055	27
$\tau_3 = \sim 30$ ms	238	2.5	0.042	32
	274	5.0	0.038	25
	368	5.0	0.043	24
	549	5.0	0.055	27
total of three steps	238	2.5	0.130	100 (117)[c]
	274	5.0	0.152	100 (70)
	368	5.0	0.180	100 (82)
	549	5.0	0.204	100 (93)

[a] Percents are based on the total ΔA_{446} observed in the experiment as determined from the SVD-deduced difference spectra as illustrated in Figure 1. The data for expt 549 are presented here and are not graphed in Figure 1. [b] Each experiment is an average of separate experiments performed sequentially on the same preparation. The numbers of separate experiments included in the averages were 17, 33, 28, and 30, respectively, for experiments 238, 274, 368, and 549. [c] The percents shown in parentheses show the percents of the total resolved ΔA_{446} referred to control experiments (cf. Figure 3) in which the magnitude of the ΔA_{446} for the total oxidation of the reduced enzyme was taken as 100%.

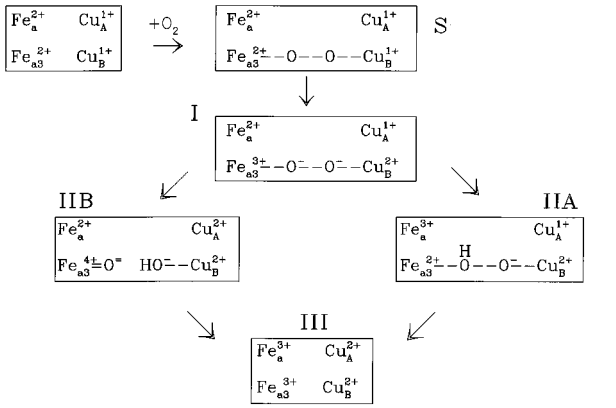

FIGURE 4: Branched sequence model. This model is based on the low-temperature electron paramagnetic resonance and optical spectroscopic studies of Clore et al. (1980) and of Chan and co-workers (Blair et al., 1985; Witt & Chan, 1987).

significance of this choice in influencing the results will be discussed at the end of this section.

The first step ($\tau \sim 0.01$ ms) in the analysis based on the branched model is the same as for the linear sequential model, namely, the binding of O_2 to the fully reduced molecule (i.e., conversion of y_1 to y_2 in the reaction scheme). The difference spectra for this step were the same as shown in Figure 1 and are not reproduced here. In the analysis of the data in the previous section, it was noted that in the first resolved kinetic step involving heme oxidation (i.e., $\tau = 90$ μs) all of the heme *a* and none of the heme a_3 were oxidized. Therefore, it could not be assigned to the first electron transfer step of the reaction sequence shown in Figure 4 (i.e., S to I). If this reaction sequence is valid, then the intermediate I (compound C) which is trapped in the cryogenic studies is not stable at room temperature, and the 90 μs transition we have isolated refers to the conversion of the fully reduced oxygen adduct, S, to the two intermediates

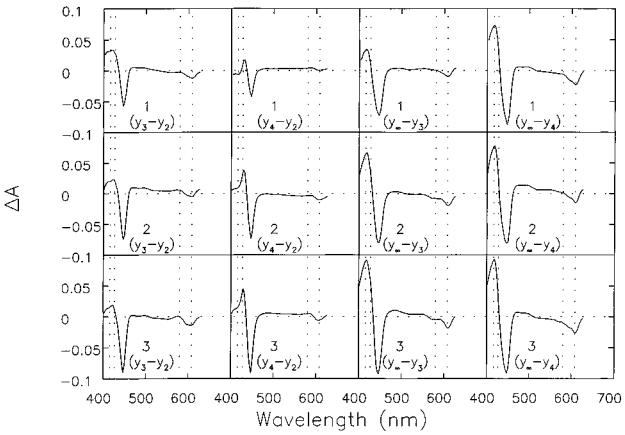

FIGURE 5: SVD-deduced difference spectra based on the branched sequence model. The SVD-derived kinetic constants were used as described in the supplementary material to obtain these difference spectra. The raw data analyzed correspond, row for row, to the same data described in the legend to Figure 1. The subscripted y terms refer to the intermediates shown in the branched reaction sequence in the text. Specifically, y_2 is the fully reduced oxygenated species, y_3 is the fast decaying branch intermediate, y_4 is the corresponding slow decaying branch intermediate, and y_∞ is the fully oxidized cytochrome aa_3.

shown as IIA and IIB in the figure. In terms of the scheme above, it is y_2 branching to y_3 and y_4. The other two isolated steps (i.e., 1.1 and 30 ms) would then be associated with the decays of intermediates IIA and IIB to III (i.e., y_∞). We arbitrarily assign the time constant for decay of 1.1 ms to the intermediate y_3 and the time constant for decay of 30 ms to the intermediate y_4. At this point, we do not try to identify y_3 or y_4 in terms of the discrete structures IIA and IIB shown in Figure 4. This will be done under Discussion. The difference spectra generated according to this analysis are shown in Figure 5.

The rows of spectra depicted in Figure 5 correspond to the same data sets described in the same rows of Figure 1. The designations (y_3-y_2), (y_4-y_2), ($y_\infty-y_3$), and ($y_\infty-y_4$) refer to SVD-resolved difference spectra between the fully reduced oxygenated starting compound, y_2 (S in Figure 4), each of the two 3-electron-reduced intermediates, y_3 and y_4 (IIB and IIA in Figure 4), and the final oxidized molecule, y_∞ (III in Figure 4). The time constant of 90 μs is associated with both the (y_3-y_2) and (y_4-y_2) difference spectra. The 1.1 and 30 ms transitions apply to the ($y_\infty-y_3$) and ($y_\infty-y_4$) difference spectra, respectively. As expected, these SVD-derived spectra differ from those depicted earlier in Figure 1 deduced for the linear sequential model. Figure 6 is provided to highlight the critical differences for the analyses of the 90 μs transition based on the two models. The solid curves show enlarged portions of the spectra obtained using the linear model in the restricted wavelength range of 550−620 nm. The dashed curves show the partial spectra obtained for the y_3-y_2 transition of the branched model for the same restricted wavelength range. This wavelength range was chosen because the presence of the suspected oxyferryl intermediate should be revealed by an enhancement of absorbance in the 570−580 nm range of the difference spectrum. The first thing to notice is that the difference in shapes for the spectra obtained by the linear and branched models is quite consistent in all cases. However, a distinct enhancement of absorbance in the 570−580 nm range, which is clearly seen in experiments 274 and 368, is

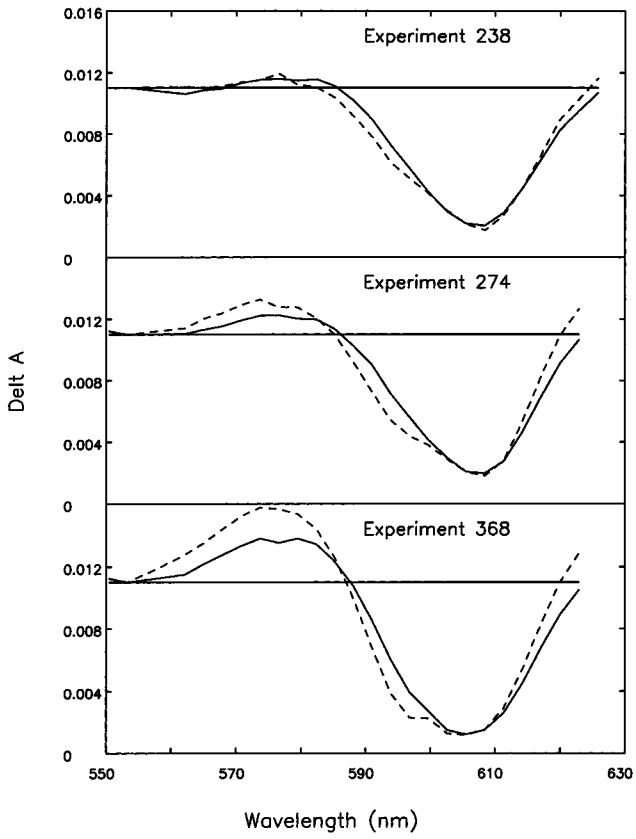

FIGURE 6: Comparison of difference spectra for the 90 μs transitions obtained using the linear sequential and branched models. The solid curves show the difference spectra obtained using the linear sequential model for the three sets of averaged kinetic experiments illustrated in Figure 1. The dashed curves show difference spectra obtained from the same data for the formation of the fast decaying branch intermediate, y_3, from the intermediate, y_2, using the branched model.

not seen in experiment 238. As mentioned earlier, experiment 238 was performed with less cytochrome aa_3 than was used in the other two cases, and fewer spectra averaged. For this reason, as discussed in the quantification analysis above, more weight is attached to the results obtained with the averaged experiments included in experiments 274 and 368.

There is one important consideration in this analysis which requires some further attention. The branching ratio for the formation of IIA and IIB from S at room temperature is not known. In the absence of this information, a branching ratio of 1:1 was assumed. The raw data which we have accumulated reflect the true branching ratio, which we will call X. If in our analysis we assigned the value $2X$ or $X/2$ to this ratio, the difference spectra produced might not correspond to any reasonable spectra expected from the heme chromophores known to be present in the cytochrome aa_3 system. In our analyses, we tried ratios of 1:2 and 2:1 in addition to 1:1. In both the 1:2 and 2:1 cases, bizarre difference spectra were obtained which had no resemblance to any difference spectra seen or expected from cytochrome aa_3. Because of this result and the fact that the 1:1 ratio produced reasonable spectra which are consistent with the resonance Raman and EPR analyses of the cytochrome aa_3 system, we believe that the 1:1 distribution is close to the actual ratio. If the true ratio at room temperature is somewhat different than 1:1, it is most likely weighted more in the direction of formation of the oxyferryl form (IIB), based on the results of Blair et al. (1985), who found a 70/

30 distribution in favor of the oxyferryl intermediate at 181 K. This would result in an underestimation for the contribution of the oxyferryl spectral component in the SVD-resolved difference spectrum using a 1:1 branching ratio.

DISCUSSION

The raw data collected at room temperature are contained in a matrix with ~66 rows (representing wavelengths) and ~1000 columns (representing individual time points in the reaction sequence). In the first phase of analysis, SVD is used to determine the number of kinetic events and their characteristic time constants, as well as a basis set of linearly independent spectral shapes (Hendler & Shrager, 1994). This deconvolution is independent of any preconceived notion of a reaction scheme or mechanism. The object of the second phase is to define the most likely kinetic sequence and to determine difference spectra between successive intermediates in the scheme. It is in this part where preconceived ideas influence the final result. We have analyzed our SVD-deduced information in terms of two different views of reaction mechanisms. Most previous kinetic studies have assumed a linear sequential series of intermediates, and this is one of the models we have tested. On the other hand, two laboratories have published a branched chain mechanism based on studies conducted at cryogenic temperatures and using a combination of electron paramagnetic resonance and optical spectroscopy (Clore et al., 1980; Blair et al., 1985). We have also analyzed our data in terms of the branched model. In interpreting both analyses, it is important to keep in mind that spectral data report only on redox states of heme centers. Unliganded, reduced hemes *a* and a_3 show maximum Soret absorbances near 446 nm. When O_2 is bound to heme a_3, these Soret absorbances are blue-shifted to about 430 nm. Similarly, the α aborbances for reduced, unliganded hemes *a* and a_3, upon O_2 binding, are blue-shifted from ~605 to ~595 nm. In the discussion that follows, the terms *free* or *liganded* heme a_3 are based on these spectral characteristics.

Analysis Based on a Linear Sequential Scheme. The complete SVD analysis has reproducibly generated four difference spectra. The fastest difference spectrum, produced within the limit of our time resolution (column 1 of Figure 1), has all of the characteristics of the oxyferrous heme species, known as compound A from the early work of Chance et al. (1975a,b). The Soret region shows the expected shift, from 446 to ~430 nm, and the α region, from ~608 to ~593 nm. As an aid to the identification of the remaining three difference spectra, we present Figure 7, which shows isolated difference spectra for cytochromes *a* and a_3, obtained by two different procedures in three different laboratories. The top panel shows reduced minus oxidized spectra obtained by Vanneste (1966), who used a combination of ligands which bind to reduced and oxidized cytochrome a_3 followed by algebraic addition and subtraction of spectra. The middle panel shows reduced minus oxidized spectra isolated by Nicholls and Wrigglesworth (1988), who used the difference in kinetic reactivities of oxidized cytochromes *a* and a_3 with dithionite. The bottom panel shows oxidized minus reduced spectra obtained in our laboratory using the same principle as Nicholls and Wrigglesworth. From all of these spectra, distinct characteristics for the difference spectra of the two cytochrome species can be discerned. In the Soret region, although the reduced species

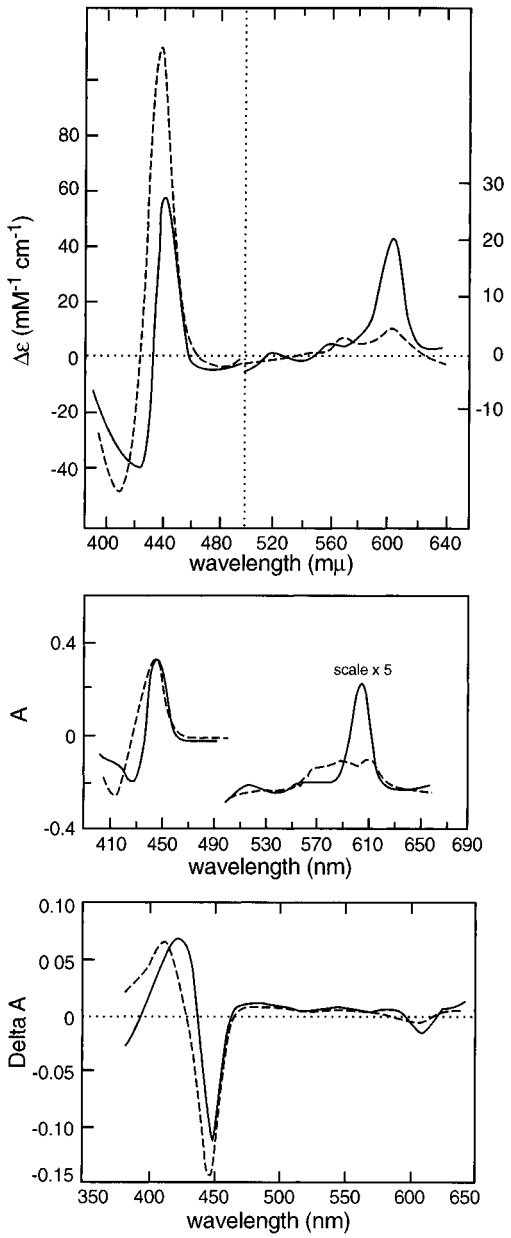

FIGURE 7: Isolated difference spectra for cytochrome *a* (solid curves) and cytochrome a_3 (dashed curves) obtained from different laboratories. Top panel: Reduced minus oxidized difference spectra obtained by Vanneste (1966) using ligands specific for hemes *a* and a_3 and algebraic combinations of spectra. Reprinted with permission of the publisher. Middle panel: Reduced minus oxidized difference spectra obtained by Nicholls and Wrigglesworth (1988) using the differences in kinetic reduction of hemes *a* and a_3 by dithionite. Reprinted with permission of the publisher. Bottom panel: Oxidized minus reduced difference spectra obtained in our laboratory using the same principle as Nicholls and Wrigglesworth.

of both cytochromes *a* and a_3 are at the same wavelength (~445 nm), the oxidized species of cytochrome *a* is near 426 nm and that of cytochrome a_3 near 414 nm. The magnitude of the Soret feature for cytochrome a_3 (445 minus 414 nm) is somewhat larger than that of cytochrome *a* (445 minus 426 nm). In the α region, there is a distinct feature for cytochrome *a* near 606 nm and a lesser, but still clear, feature in the 570−590 nm region. Cytochrome a_3 shows smaller and less distinct features in the 550−620 nm region.

An examination of the difference spectrum isolated by SVD for the species with τ ~90 μs (column 2 of Figure 1) shows that it looks very much like the isolated difference

spectrum for cytochrome *a* (Figure 7). The reduced Soret peak at 446 nm is balanced by an oxidized peak at ~427 nm. There is a distinct α feature at ~606 nm and a clear "hump" near 580 nm. The feature near 580 nm is at or above the zero line just as seen in the spectra for cytochrome *a* shown in the panels of Figure 7. The other two difference spectra isolated by SVD (columns 3 and 4 in Figure 1) look much more like the isolated spectra for cytochrome a_3. The reduced Soret peak at 446 nm is compensated by an oxidized peak near 416 nm. There is less distinction for a feature near 580 nm, and the absorbance near 580 nm is more negative than that seen in the spectra in column 2 of Figure 1 and for the isolated cytochrome *a* spectra in Figure 7. It much more closely resembles the difference spectrum for cytochrome a_3 (Figure 7). The resemblance of the spectra in columns 3 and 4 of Figure 1 to the isolated spectra for cytochrome a_3, however, is not absolute. Although the shape of the α feature resembles that of the α feature for cytochrome a_3, its magnitude relative to the Soret feature is distinctly greater than that seen for the isolated cytochrome a_3. A likely explanation for this difference is that O_2 is bound to the enzyme in the spectra shown in Figure 1 but not in Figure 7. On the basis of the considerations discussed above, we believe that the difference spectrum with a τ near 10 μs represents the formation of a ferrous heme a_3-O_2 liganded species, the difference spectrum with a τ near 90 μs represents the oxidation of heme *a*, and the latter two difference spectra represent two stages in the oxidation of heme a_3.

Therefore, this approach has isolated three steps in which electrons leave cytochrome aa_3. Using the magnitude of the change in absorbance at 446 nm as a measure of heme oxidation and comparing the total amount of this change for the three isolated steps to the total amount of change for the complete reduction of cytochrome aa_3 by dithionite, we are able to account essentially for the complete oxidation of the reduced enzyme (Table 1).

The most directly comparable data are those of Orii, who obtained complete optical spectra at room temperature for both the Soret and α absorbance regions (Orii, 1984,1988). His difference spectra in both regions are virtually identical to our resolved spectra for the same time domains. Other published spectra were obtained under cryogenic conditions (Chance et al., 1975a,b; Clore et al., 1980). There is agreement in all of these studies that only in the case of the earliest (primary) intermediate are the characteristic absorbance features for liganded heme a_3 seen. All later intermediates show absorbance features more characteristic of unliganded heme a_3. This is evident in both the SVD-derived spectra and the actual difference spectra and, as discussed above, is in agreement with published spectra from other laboratories. This suggests that the oxygen$-Cu_B$ liganding is stronger than that of oxygen$-Fe_{a3}$. In this context, it should be noted that Blair et al. (1985) interpreted their electron paramagnetic resonance data for the 3-electron-reduced peroxy species to indicate that the oxygen is strongly anchored to the Cu_B and either weakly exchange- or dipolar-coupled to a reduced but intermediate spin ferrous heme. They estimated that this species accounted for 60−70% of the bound peroxide.

Quantification of the extents of spectral changes at 446 nm indicates that ~50, ~25, and ~25% oxidation occurred, respectively, in these three steps (Table 1). The first step

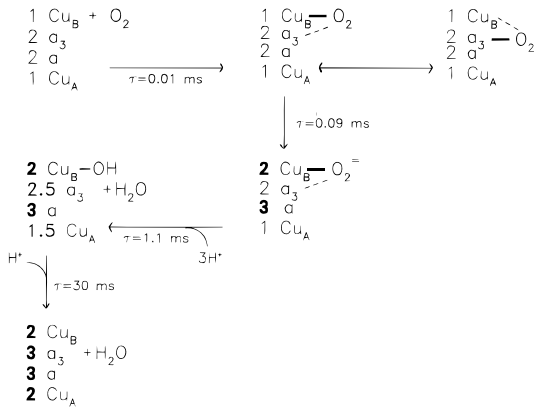

FIGURE 8: Reaction scheme consistent with SVD analysis based on the linear sequential scheme. The numbers show the valence of each redox-active metal center in cytochrome aa_3. The reduced state of the metal center is indicated by the light typeface of the number. The fully oxidized state is indicated by the thick typeface and the partially reduced state by an intermediate thickness. The time constants shown correspond to the ones deduced by SVD and shown in Figure 1 and Table 1. The heavy (solid) and light (dashed) bonds shown as ligands to oxygen are based on the observed difference spectra for heme a_3 oxidation and the electron paramagnetic resonance results of Blair et al. (1985), as discussed in the text.

was identified (above) as the oxidation of heme *a*, which accounts for 50% of the total heme. Therefore, the event with τ near 0.1 ms appears to be the complete oxidation of heme *a*. The next two steps (τ's of ~1.1 and 30 ms) were identified (above) as involving the oxidation of heme a_3. The quantification in Table 1 is consistent with two successive electron transfer steps.

It is expected that the first step in O_2 reduction involves a two-electron reduction of the bound O_2 to a peroxy intermediate (Wikström et al., 1981; Brunori et al., 1988; Hill et al., 1986). We interpret the first step as involving two near-simultaneous events; first, the transfer of two electrons from Cu_B and heme a_3 to O_2; and second, the rapid transfer of an electron from heme *a* to heme a_3. To account for the apparent two-step reduction of the heme a_3 center, we propose (Figure 8) coupled transfers involving the heme a_3 and Cu_A centers. We know of no evidence specifically linking these centers, and this explanation is admittedly speculative. A very recent paper by Yoshikawa et al. (1994) points to a sharing of electrons among the redox-active metal centers.

The scheme presented in Figure 8 is compatible with the analysis based on a linear sequential scheme of intermediates. To account for the observation that the difference spectra for cytochrome a_3 resemble the unliganded form, compound A is shown as a side reaction. Alternatively, it may be considered that electron passage to bound O_2 occurs most readily when the oxygen is bound tightly to Cu_B as in the peroxy compound described below in connection with the branched chain model.

Analysis Based on a Branched Sequential Scheme. An important difference between the linear sequential and the branched chain analyses is that only a single difference spectrum is obtained for the 90 μs transition in the former case, but two are obtained in the latter. Up to this point, we have not tried to identify the intermediates, y_3 and y_4, in terms of the particular compounds IIA and IIB, described by Chan and his co-workers. Compound IIB is an oxyferryl species with both copper centers oxidized and heme *a*

remaining in the reduced state. In compound IIA, Cu_A and heme a_3 are in the reduced states, while heme *a* and Cu_B are oxidized. In considering the likely difference spectra between the starting compound and each of these suspected intermediates, the fact that heme *a* oxidation is expected in the formation of IIA but not IIB is important. An additional consideration is that the formation of the oxyferryl intermediate is correlated with the lack of oxidation of heme *a*. Oxidized heme *a* has a prominent Soret absorption at ~427 nm. The oxyferryl compound is characterized by absorbance features at ~580 and ~530 nm (Witt & Chan, 1987; Vygodina & Konstantinov, 1988). Difference spectra obtained by Vygodina and Konstantinov upon addition of first 30 μM and then 3 mM H_2O_2 to oxidized cytochrome aa_3 liposomes at pH 7.5 are reproduced in the upper panel of Figure 9. The dashed curves are taken as representative of the formation of the peroxy complex and the solid as representative of the oxyferryl state. In the bottom panel are similar difference spectra, except for the facts that the pH was 8.0, the lower concentration of peroxide was 20 μM (curves a), and 100 μM ferricyanide was present before the addition of H_2O_2. The dashed curves show the base lines, and curve b obtained at 3 mM H_2O_2 is interpreted as representing the formation of the oxyferryl state. Based on all of the considerations stated above and these representative spectra as well as similar observations of Witt and Chan (1987), the difference spectra (y_3-y_2) shown in Figures 5 and 6 look like the formation of compound IIB from the fully reduced molecule. The relative prominence of the positive difference near 580 nm in relation to the negative difference at ~607 nm is consistent with the formation of an oxyferryl species. One of the problems in identifying the presence of the oxyferryl species is the small extinction coefficient for the positive absorbance in the near 580 nm absorbance region and the fact that this absorbance must be distinguished from the hump in absorbance that is present in the difference spectrum for cytochrome *a* (cf. Figure 7). The difference spectra for the formation of the oxyferryl state from the oxidized enzyme (Figure 9, top panel, solid line) and for the oxidation of reduced cytochrome *a* (Figure 7, bottom panel, solid line) are quite comparable in shape in the 550−630 nm range. The only difference appears to be an enhanced positive absorbance near 580 nm relative to the trough at ~607 nm compared to the cytochrome *a* oxidation difference spectrum. When the two spectra are present together, the height at ~580 nm relative to the trough at ~607 nm will be a weighted average of the two individual spectra. A direct comparison of the spectra obtained for the 90 μs transition using the linear sequential model and the (y_3-y_2) spectra using the branched model (Figure 6) shows that the absorbance spectra for the branched model generally show an enhancement in absorbance in the 570−580 nm region compared to the linear model. The apparent absence of the other characteristic positive difference feature at ~530 nm is explained by the fact that the region from 516 to 550 nm was blocked out to avoid interference from the ND:YAG laser at 532 nm. The difference spectrum (y_4-y_2) is compatible with the changes in redox states expected for the formation of compound IIA from the fully reduced molecule. Consistent with these interpretations is the appearance of a negative difference at ~580 nm in the ($y_\infty-y_3$) spectra. This is expected for the decay of the oxyferryl state. The strong positive Soret at ~416 nm in both the ($y_\infty-y_3$) and ($y_\infty-y_4$) difference spectra is compatible with the final formation of ferric heme a_3.

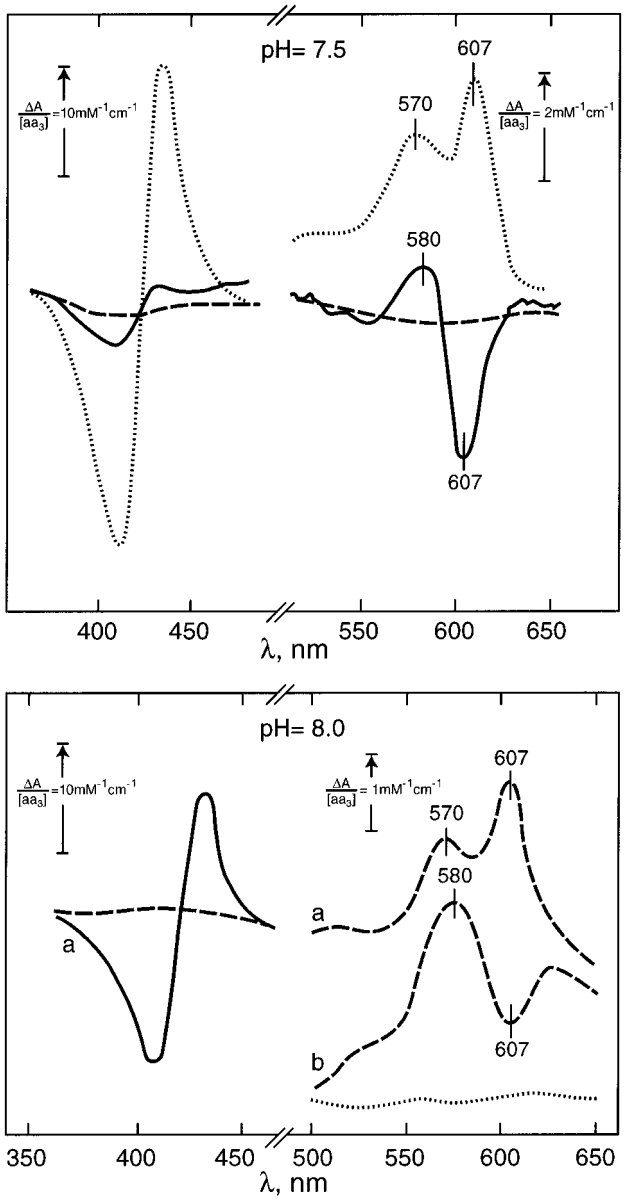

FIGURE 9: Isolated difference spectra for formation of peroxy and oxyferryl complexes from cytochrome aa_3 by addition of H_2O_2. These figures are reprinted from the article by Vygodina and Konstantinov (1988) with permission of the publisher. The top panel shows the formation of the putative peroxy complex by the addition of 30 μM H_2O_2 to oxidized cytochrome aa_3 liposomes at pH 7.5 (dotted lines), and then the formation of the putative oxyferryl state by further addition 3 mM H_2O_2 to the cuvette (solid lines). The bottom panel shows the formation of the same two H_2O_2-induced states at pH 8.0 by the addition of 20 μM (curve a) and 3 mM (curve b) H_2O_2 to ferricyanide-treated cytochrome aa_3 liposomes at pH 8.0. The dashed curves in both panels represent background lines.

Evaluation of the Two Different Analyses in Terms of Other Published Data. Table 2 presents a summary of kinetic steps that have been resolved in other laboratories in studies performed at room temperature. All of the analyses from these laboratories were based on optical absorption, utilizing single-wavelength data, except that of Varotsis et al. (1993), who used resonance Raman spectroscopy. As to the identity of the intermediates involved, there is essentially no agreement except for the following two points. The first step, prior to actual transfer of electrons to O_2, is that O_2 is

Table 2: Time Constants Derived from Room Temperature Studies

ref	1[b]	2	3[c]	4[d]	5	6	T[e]
Gibson & Greenwood (1965), Greenwood & Gibson (1967)	0.03[a]	0.14			1.25		1
Hill & Greenwood (1984)	0.03 0.05	0.14			1.25		1
Oliveberg et al. (1989)	0.04	0.10			1.25		1
Varotsis et al. (1993)	<0.03	0.10	0.17	0.83	1.25		2
Hill (1994)	0.05	0.13			1.67		1
this paper	0.09				1.1	30	3

[a] All data are expressed in time constants (τ) in milliseconds, and they represent electron transfer events in the oxidation of cytochrome aa_3 heme groups by O_2. [b] The step represented in column 1 is identified as the 2-electron reduction of bound O_2 to bound peroxide. [c] This step is identified with the formation of the ferryl form of heme a_3. [d] This step is identified with the decay of the ferryl form of heme a_3. [e] The technique for data acquisition and analysis: (1) single-wavelength absorption data and fitting to sums of exponentials; (2) consideration of time-resolved resonance Raman spectra; (3) singular value decomposition analysis of multichannel optical absorption data covering both the Soret and α regions.

bound to the reduced heme a_3 center and that this step is so fast that it has not been resolved, except in the studies of Orii (1988), who provide evidence in a difference spectrum in the time range of 5−20 μs, and in our studies reported in this paper. The second step, which is the first involved in O_2 reduction, involves two electrons, and results in the formation of a bound peroxy intermediate. The data in column 1 of Table 2 represent the step attributed to the formation of the peroxy intermediate. The agreement on these two points also applies to the low-temperature studies. It should be noted that our τ for this step is somewhat larger than previous values. Other studies using optical absorbance data have implicated a step with a τ of ∼120 μs. Varotsis et al. (1993) include τ's of ∼170 and ∼830 μs, derived from resonance Raman studies, which they attribute to the formation and dissipation of the oxyferryl intermediate. All laboratories, including ours, see a step with a τ close to 1 ms. Our work implicates a step with a $\tau = \sim$30 ms. This time constant is consistent with the measured turnover of the enzyme which is close to 40 s^{-1}. We find that the ΔA_{446} represented in this transition is essential in accounting for the total oxidation of the cytochrome aa_3. Other studies have not examined this extended time range and have not provided quantitative data to account for the total oxidation of the enzyme.

There is one major difference in the results of the linear sequential and branched chain analyses of the SVD-derived data. The linear sequential analysis yielded no clear support for a major role of an oxyferryl intermediate whereas the branched chain analysis did. Many laboratories have proposed an oxyferryl intermediate during the oxidation of reduced cytochrome aa_3 by O_2 (Chance et al., 1975b; Wikström, 1981, 1989; Orii, 1988; Babcock & Wikström, 1992; Blair et al., 1985; Witt & Chan, 1987).

In recent years, resonance Raman studies have added strong support to this view (Varotsis et al., 1993; Ogura et al., 1990; Han et al., 1990). According to Varotsis et al. (1993), we would expect to see a difference spectrum for the formation of this species with a τ of ∼166 μs and a difference spectrum for its disappearance with a τ of ∼833 μs. In the linear sequential analysis, we do not see these transitions, and we can account for the complete oxidation of the reduced enzyme in the three transitions isolated by this analysis. The difference spectrum for the 90 μs transition obtained in the linear sequence analysis (Figure 1) shows a small positive difference at ∼580 nm on the side of a deep trough at ∼607 nm. The same difference spectrum has been seen by Orii (1988) and Einarsdóttir et al. (1995) and has been cited in favor of the formation of the oxyferryl intermediate. We consider this as scant evidence, however, because essentially the same spectrum is seen in the oxidized minus reduced difference spectrum for cytochrome *a*. In the linear sequence analysis, this difference spectrum is consistent with the oxidation of heme *a* and formation of the peroxy intermediate shown in Figure 8. In a recent preliminary communication, Sucheta et al. (1996) reported that an SVD analysis (based on a linear sequential model) of spectral, kinetic data obtained during the oxidation of fully reduced cytochrome aa_3 by O_2 yielded five time constants: 1, 15, 30, and 80 μs and 1.2 ms. They attributed these, respectively, to a conformational change at a_3, formation of compound A, oxidation of heme *a*, formation of an oxyferryl intermediate, and the oxidation of heme a_3. Except for the 1 μs process and the attribution of the ∼80 μs process to an oxyferryl compound, these results are quite similar to our linear sequential analysis reported in this paper and earlier (Bose & Hendler, 1995).

The results of the branched chain analysis are consistent with the resonance Raman data. In place of the single difference spectrum for the 90 μs transition, we obtain two different spectra for the formation of each of the suspected 3-electron-reduced intermediates. In one of them, the positive feature at 580 nm is more prominent in relation to the negative feature at ∼607 nm than that seen either in the isolated oxidized minus reduced cytochrome *a* spectrum (Figure 7) or in the single difference spectrum shown in Figure 1. As discussed above, the other difference spectra obtained in this analysis are also compatible with the resonance Raman data. The SVD-based analysis of the branched reaction scheme mechanism is compatible with both the EPR and resonance Raman data that have been obtained.

Final Thoughts. Although the single-turnover kinetics of cytochrome aa_3 oxidation by O_2 have been traditionally analyzed in terms of a linear sequence of intermediates, the results of our multichannel analysis, based on singular value decomposition, present several unexpected results, the most disturbing of which is that no direct support for the existence of a major oxyferryl intermediate was obtained. From this, it could be argued that the variety of physical techniques which have found evidence for such an intermediate suffer from their lack of quantification that is needed to firmly establish that an oxyferryl compound is a direct obligatory intermediate. On the other hand, from a theoretical consideration of the possible routes of electron transfer in a molecule that offers more than a single possibility and in view of direct physical evidence for a branched pathway, the direct linear sequential scheme may be a less appropriate model for evaluating the accumulated data. The finding that the analysis based on the previously suggested branched model presents a picture in complete agreement with the many cited EPR and resonance Raman studies which have implicated the oxyferryl intermediate adds strong support in favor of a branched pathway for the route of electron transfer from fully reduced cytochrome aa_3 to O_2.

SUPPORTING INFORMATION AVAILABLE

General description of the methods used to model SVD-derived eigenvectors of spectral and kinetic properties into sequential, linear, and branched reaction pathways. Of particular importance are the derivations and presentation of kinetic matrices used to deduce individual difference spectra for each kinetic step in both models (6 pages). Ordering information is available on any current masthead page.

REFERENCES

Babcock, G. T., & Wikström, M. (1992) *Nature (London) 356*, 301−309.

Blackmore, R. S., Greenwood, C., & Gibson, Q. H. (1991) *J. Biol. Chem. 266*, 19245−19249.

Blair, D. F., Witt, S. N., & Chan, S. I. (1985) *J. Am. Chem. Soc. 107*, 7389−7399.

Bose, S., & Hendler, R. W. (1995) *Biophys. J. 68*, A319.

Brunori, M., Antonini, G., Malatesta, F., Sarti, P., & Wilson, M. T. (1988) *Adv. Inorg. Chem. 7*, 93−153.

Chance, B., Saronio, C., & Leigh, J. S., Jr. (1975a) *Proc. Natl. Acad. Sci. U.S.A. 72*, 1635−1640.

Chance, B., Saronio, C., & Leigh, J. S., Jr. (1975b) *J. Biol. Chem. 250*, 9226−9237.

Clore, M., Andreasson, L.-E., Karlsson, B., Aasa, R., & Malmström, B. G. (1980) *Biochem. J. 185*, 139−154.

Crinson, M., & Nicholls, P. (1991) *Biochem. Cell Biol. 70*, 301−308.

Einarsdóttir, O., Choc, M. G., Weldon, S., & Caughey, W. S. (1988) *J. Biol. Chem. 263*, 13641−13654.

Einarsdóttir, O., Sucheta, A., & Georgiadis, K. E. (1995) *Biophys. J. 68*, A323.

Gibson, Q. H., & Greenwood, C. (1963) *Biochem. J. 86*, 541−554.

Gibson, Q. H., & Greenwood, C. (1965) *J. Biol. Chem. 240*, 2694−2698.

Greenwood, C., & Gibson, Q. H. (1967) *J. Biol. Chem. 242*, 1782−1787.

Han, S., Ching, Y., & Rousseau, D. L. (1990) *Nature 348*, 89−90.

Hazzard, J. T., Rong, S., & Tollin, G. (1991) *Biochemistry 30*, 213−222.

Hendler, R. W., & Shrager, R. I. (1994) *J. Biochem. Biophys. Methods 28*, 1−33.

Hendler, R. W., Bose, S. K., & Shrager R. I. (1993) *Biophys. J. 65*, 1307−1317.

Hill, B. C. (1994) *J. Biol. Chem. 269*, 2419−2425.

Hill, B. C., & Greenwood, C. (1984) *Biochem. J. 218*, 913−921.

Hill, B. C., Greenwood, C., & Nicholls, P. (1986) *Biochim. Biophys. Acta 853*, 91−113.

Ishibe, N., Lynch, S. R., & Copeland, R. A. (1991) *J. Biol. Chem. 266*, 23916−23920.

Malatesta, F., Sarti, P., Antonini, G., Vallone, B., & Brunori, M. (1990) *Proc. Natl. Acad. Sci. U.S.A. 87*, 7410−7413.

Morgan, J. E., Li, P. M., Jang, D.-J., Sayed, M. A., & Chan, S. I. (1989) *Biochemistry 28*, 6975−6983.

Nagle, J. F., Parodi, L. A., & Lozier, R. H. (1982) *Biophys. J. 38*, 161−174.

Nicholls, P., & Wrigglesworth, J. M. (1988) *Ann. N.Y. Acad. Sci. 550*, 59−67.

Ogura, T., Takahashi, S., Shinzawa-Itoh, K., Yoshikawa, S., & Kitigawa, T. (1990) *J. Biol. Chem. 265*, 14721−14723.

Oliveberg, M., Brzezinski, P., & Malmström, B. G. (1989) *Biochim. Biophys. Acta 977*, 322−328.

Orii, Y. (1984) *J. Biol. Chem. 259*, 7187−7190.

Orii, Y. (1988) *Ann. N.Y. Acad. Sci. 550*, 105−117.

Pardhasaradhi, K. B., Ludwig, K. B., & Hendler, R. W. (1991) *Biophys. J. 60*, 408−414.

Sinjorgo, K. M., Steinebach, O. M., Dekker, H. L., & Muijsers, A. O. (1986) *Biochim. Biophys. Acta 850*, 108−115.

Sucheta, A., & Einarsdóttir, O. (1996) *Biophys. J. 70*, A343.

Vanneste, W. H. (1966) *Biochemistry 5*, 838−848.

Varotsis, C., Zhang, Y., Appelman, E. H., & Babcock, G. T. (1993) *Proc. Natl. Acad. Sci. U.S.A. 90*, 237−241.

Vygodina, T. V., & Konstantinov, A. A. (1988) *Ann. N.Y. Acad. Sci. 550*, 124−138.

Wikström, M. K. (1981) *Proc. Natl. Acad. Sci. U.S.A. 78*, 4051−4053.

Wikström, M. K. (1989) *Nature (London) 338*, 776−778.

Wikström, M. K., Krab, K., & Saraste, M. (1981) *Cytochrome oxidase. A synthesis*, 198 pp, Academic Press, New York.

Wilms, J., Van Rijn, J. L. M. L., & Van Gelder, B. V. (1980) *Biochim. Biophys. Acta 593*, 17−23.

Witt, S. N., & Chan, S. I. (1987) *J. Biol. Chem. 262*, 1446−1448.

Wrigglesworth, J. M. (1984) *Biochem. J. 217*, 715−719.

Yoshikawa, S., Choc, M. G., O'Toole, M. C., & Caughey, W. S. (1977) *J. Biol. Chem. 252*, 5498−5508.

Yoshikawa, S., Mochizuki, M., Zhao, X.-J., & Caughey, W. S. (1994) *J. Biol. Chem.* (submitted for publication).

BI9617419